



Characterization of the interaction between lysyl-tRNA synthetase and laminin receptor by NMR



Hye Young Cho^a, Ameerq Ul Mushtaq^a, Jin Young Lee^b, Dae Gyu Kim^b, Min Sook Seok^a, Minseok Jang^c, Byung-Woo Han^c, Sunghoon Kim^b, Young Ho Jeon^{a,*}

^a College of Pharmacy, Korea University, 2511 Sejong-ro, Sejong 339-700, Republic of Korea

^b Medicinal Bioconvergence Research Center, College of Pharmacy, Seoul National University, Seoul 151-742, Republic of Korea

^c Research Institute of Pharmaceutical Sciences, College of Pharmacy, Seoul National University, Seoul 151-742, Republic of Korea

ARTICLE INFO

Article history:

Received 4 April 2014

Revised 30 May 2014

Accepted 11 June 2014

Available online 28 June 2014

Edited by Christian Griesinger

Keywords:

Lysyl-tRNA synthetase

Laminin receptor

Nuclear magnetic resonance

Laminin

ABSTRACT

Lysyl-tRNA synthetase (KRS) interacts with the laminin receptor (LR/RPSA) and enhances laminin-induced cell migration in cancer metastasis. In this nuclear magnetic resonance (NMR)-based study, we show that the anticodon-binding domain of KRS binds directly to the C-terminal region of 37LRP, and the previously found inhibitors BC-K-01 and BC-K-YH16899 interfere with KRS–37LRP binding. In addition, the anticodon-binding domain of KRS binds to laminin, observed by NMR and SPR. These results provide crucial insights into the structural characteristics of the KRS–LR interaction on the cell surface.

Structured summary of protein interactions:

KRS-ABD binds to **37LRP** by surface plasmon resonance (View interaction)

KRS-ABD and **37LRP** bind by nuclear magnetic resonance (1, 2, 3)

37LRP and **KRS-ABD** bind by molecular sieving (View interaction)

KRS-ABD and **laminin peptide** bind by nuclear magnetic resonance (View interaction)

© 2014 Published by Elsevier B.V. on behalf of the Federation of European Biochemical Societies.

1. Introduction

Aminoacyl-tRNA synthetases (ARSs) play a central role in protein synthesis by catalyzing the aminoacylation of tRNAs with corresponding amino acids. Besides their canonical function in protein synthesis, mammalian ARSs play additional roles, performing diverse cellular functions [1,2]. The so-called non-canonical functions of ARSs are often performed by additional domains, which are not necessarily involved in the catalytic activities of the enzyme. The pathophysiological involvement of ARSs in various human diseases, including cancer and immune diseases,

was recently reported [3–5]. In higher eukaryotic organisms, almost half of all cellular tRNA synthetases form a multi-tRNA synthetase complex (MSC) with three non-enzymatic cofactors [6,7]. The association and dissociation of these MSC components is considered to be one of the underlying mechanisms that drive the non-canonical functions of ARSs [8–11].

Among the ARSs, lysyl-tRNA synthetase (KRS) is a multi-functional enzyme, which, in addition to its primary function of aminoacylation of lysine onto the cognate tRNA, has various non-canonical functions [12–17]. KRS is secreted from intact human cells in response to tumor necrosis factor α (TNF- α) stimulation and enhances macrophage migration [17], and KRS expression and its association with the assembly mechanism of human immunodeficiency virus type 1 (HIV-1) is responsible for HIV-1 infectivity [18]. Furthermore, KRS is a major source of diadenosine tetraphosphate (Ap4A) in immunologically activated mast cells, and via translocation into the nucleus, KRS controls the expression of microphthalmia-associated transcription factor (MITF)-inducible genes in allergic responses [12].

KRS was recently shown to induce cancer cell migration through its interaction with the 67-kDa laminin receptor (67LR)

Abbreviations: KRS, lysyl-tRNA synthetase; LR, laminin receptor; RPSA, ribosomal protein SA; 37LRP, 37 kDa laminin receptor precursor; 67LR, 67 kDa laminin receptor; NMR, nuclear magnetic resonance; TROSY, transverse relaxation optimized spectroscopy; GST, glutathione S-transferase; SUMO, small ubiquitin-like modifier; TRX, thioredoxin; MAPK, mitogen-activated protein kinase; HEPES, 4-(2-hydroxyethyl)-1-piperazineethanesulfonic acid; PMSF, phenylmethylsulfonyl fluoride; DTT, dithiothreitol; MITF, microphthalmia-associated transcription factor; Ap4A, diadenosine tetraphosphate

* Corresponding author.

E-mail address: yhjeon@korea.ac.kr (Y.H. Jeon).

[15]. LR/RPSA (HGNC: 6502) is a non-integrin cell-surface receptor with a high affinity for laminin and is known to be a key player in tumor invasion and metastasis [19]. LR/RPSA has a putative transmembrane segment, and the C-terminal region of LR/RPSA interact with the laminin in the extracellular matrix [20]. 67LR is produced in the cell by dimerization and fatty acid acylation of the 37-kDa cytosolic laminin receptor precursor (37LRP), but it is not clear whether 67LR is a homodimer or a heterodimer with a protein related to galectin-3 [20–22]. In laminin signaling, KRS is phosphorylated at Thr52 by p38 mitogen-activated protein kinase (MAPK), after which KRS translocates to the plasma membrane. The interaction of KRS with 67LR enhances the membrane stability of 67LR, which in turn results in an increase in metastasis [15].

The three-dimensional (3D) structures of KRS (residues 70–581) and N-terminal domain of 37LRP (residues 1–220) have been solved by X-ray crystallography [9,10,23]. The structure of the membrane-embedded 67LR, however, and the precise mechanism underlying the formation of 67LR is not clear [20]. The observation that 37LRP and 67LR share several functions, in particular the binding of laminin, suggests that their structures and folding states are rather similar [24]. Co-immunoprecipitation and pull-down assays have shown the interaction between KRS and LR/RPSA to occur via the N-terminal region of KRS (residues 1–219) and the transmembrane and extracellular domain (residues 88–295) of LR/RPSA [15]. A structural analysis of human KRS indicated that residues 72–207 form the anticodon-binding domain, and residues 221–576 form the catalytic domain (PDB 3BJU) [9]. To further understand the structural characteristics of the interaction between KRS and LR/RPSA, we investigated the interaction between the N-terminal region of KRS (residues 1–207) and full-length 37LRP (1–295) using nuclear magnetic resonance (NMR). The interaction was assessed in the presence and absence of a laminin peptide (DPGYIGSR). These studies provide critical insight into the structural characteristics of the KRS–LR interaction in the cell membrane.

2. Materials and methods

Detailed description of sample preparation and supporting analyses can be found in the [Supplemental methods](#).

2.1. NMR spectroscopy

To identify the NMR signals from the anticodon-binding domain and the N-terminal extension of KRS, ^1H – ^{15}N transverse relaxation optimized spectroscopy (TROSY) experiments for 0.2 mM ^{15}N -labeled KRS-Nex (residues 1–72), KRS-ABD (residues 72–207), and KRS- ΔC (residues 1–207) were measured and analyzed. The backbone assignments of ^{13}C - and ^{15}N -labeled KRS-Nex and KRS-ABD were performed using conventional triple-resonance, HNCA, HN(CO)CA, HNCACB, CBCA(CO)NH, HNCO, HN(CA)CO, HBHANH and HBHA(CO)NH experiments. Data were processed with NMRpipe [25] and analyzed with CCPN2.1.5 [26]. All NMR spectra were recorded using an Avance 600 MHz NMR spectrometer equipped with a triple-resonance probe (Bruker, Germany).

For the binding study of KRS, a series of ^1H – ^{15}N TROSY experiments of 0.2 mM ^{15}N -labeled KRS- ΔC (residues 1–207) with its binding partners were carried out in a buffer containing 20 mM HEPES (pH 7.0), 100 mM NaCl, 1 mM phenylmethylsulfonyl fluoride (PMSF) and 1 mM DTT at 30 °C as following. To characterize the interaction between KRS and LR, glutathione S-transferase (GST)-fused full length 37LRP (GST-LR) was added serially to final concentrations of 0.02, 0.03, 0.06, 0.10, 0.12, 0.16 and 0.20 mM to 0.2 mM ^{15}N -labeled KRS- ΔC . 0.2 mM free GST was used instead of GST-LR for control experiment. To identify the binding region

of LR for KRS binding, small ubiquitin-like modifier (SUMO)-fused 37LRP fragments (residues 1–295: SUMO-LR_{full}; residues 1–86: SUMO-LR_{1–86}; residues 1–209: SUMO-LR_{1–209}; residues 86–295: SUMO-LR_{86–295}; and residues 102–295: SUMO-LR_{102–295}; residues 210–295: SUMO-LR_{210–295}) were constructed and expressed. The SUMO tag was cleaved off for the LR_{1–209}, LR_{102–295}, LR_{210–295} and LR_{full} before NMR study. Then, 0.2 mM of each tag-free LR_{full}, LR_{1–209}, LR_{102–295}, LR_{210–295}, SUMO-LR_{1–86}, SUMO-LR_{86–295}, and SUMO-LR_{102–295} were added to 0.2 mM ^{15}N -labeled KRS- ΔC , respectively (1:1 ratio). To see the effect of laminin peptide, 0.3 mM laminin peptide was added to 0.2 mM ^{15}N -labeled KRS- ΔC in the absence and presence of 0.06 mM GST-LR. For the binding of thioredoxin-fuse 37LRP (TRX-LR) with KRS-ABD, 0.2 mM TRX-LR was added to 0.2 mM ^{15}N -labeled KRS-ABD (residues 72–207) in the presence of 20 mM arginine.

2.2. Modeling of full length KRS

Since the X-ray structure of the KRS anticodon-binding and catalytic domains (residues 70–579) has been reported (PDB: 3BJU), the full-length KRS structural model was prepared from two template structures: the N-terminal (residues 1–72) structure was derived from chemical shift data with CYANA2.1 (<http://www.las.jp/english/products/cyana.html>) and the X-ray structure of the anticodon-binding and catalytic domains was used as templates for the rest of the protein. For the CYANA calculation, angular restraints from TALOS (<http://spin.niddk.nih.gov/bax/software/TALOS/>) based on ^1H , $^{13}\text{C}_\alpha$, $^{13}\text{C}_\beta$, $^{13}\text{C}'$ chemical shift data of KRS-Nex were used. Modeling was performed using Modeller4 (<http://salilab.org/modeller>), and the structure quality was accessed with RAMPAGE, a public domain webserver (<http://mordred.bioc.cam.ac.uk/~rapper/rampage.php>).

3. Results and discussion

3.1. Identification of NMR signals from the flexible N-terminal extension and anticodon-binding domain

We have already reported that the N-terminal region (1–219) of KRS binds with 37LRP and 67LR in vitro [15]. Human KRS has three functional domains: an N-terminal extension (residues 1–72), an anticodon-binding domain (residues 72–207), and a catalytic domain (residues 220–597) ([Supplemental Fig. 1A](#)). Only mammalian KRS contains a flexible N-terminal extension, which provides additional tRNA binding affinity [27]. In order to identify the NMR signals that correspond to each region of the N-terminal extension and anticodon-binding domain, we prepared purified KRS fragments containing the residues 1–72 (KRS-Nex), 72–207 (KRS-ABD), and 1–207 (KRS- ΔC) ([Supplemental Fig. 1B and D](#)) and performed ^1H – ^{15}N TROSY NMR experiments ([Supplemental Fig. 1E and F](#)). Interestingly, most of the NMR signals of KRS-Nex and KRS-ABD ([Supplemental Fig. 1F](#), blue and red color, respectively) were closely matched with the signals from the spectrum of KRS- ΔC ([Supplemental Fig. 1E and black color of 1F](#)). This result is indicative of independent motion between the residues corresponding to the N-terminal extension and the anticodon-binding domain in the KRS- ΔC protein, showing that the two domains do not interact with each other. Thus, we were able to identify the NMR signals from these individual domains separately. Next, the backbone resonances of KRS-Nex and KRS-ABD were assigned using conventional triple-resonance NMR experiments ([Supplemental Fig. 2A and B](#), BMRB Accession Nos. 19993 and 19995, respectively). Using this information, an NMR binding study of KRS and GST-LR was performed to allow the domain of KRS responsible for the interaction to be identified.

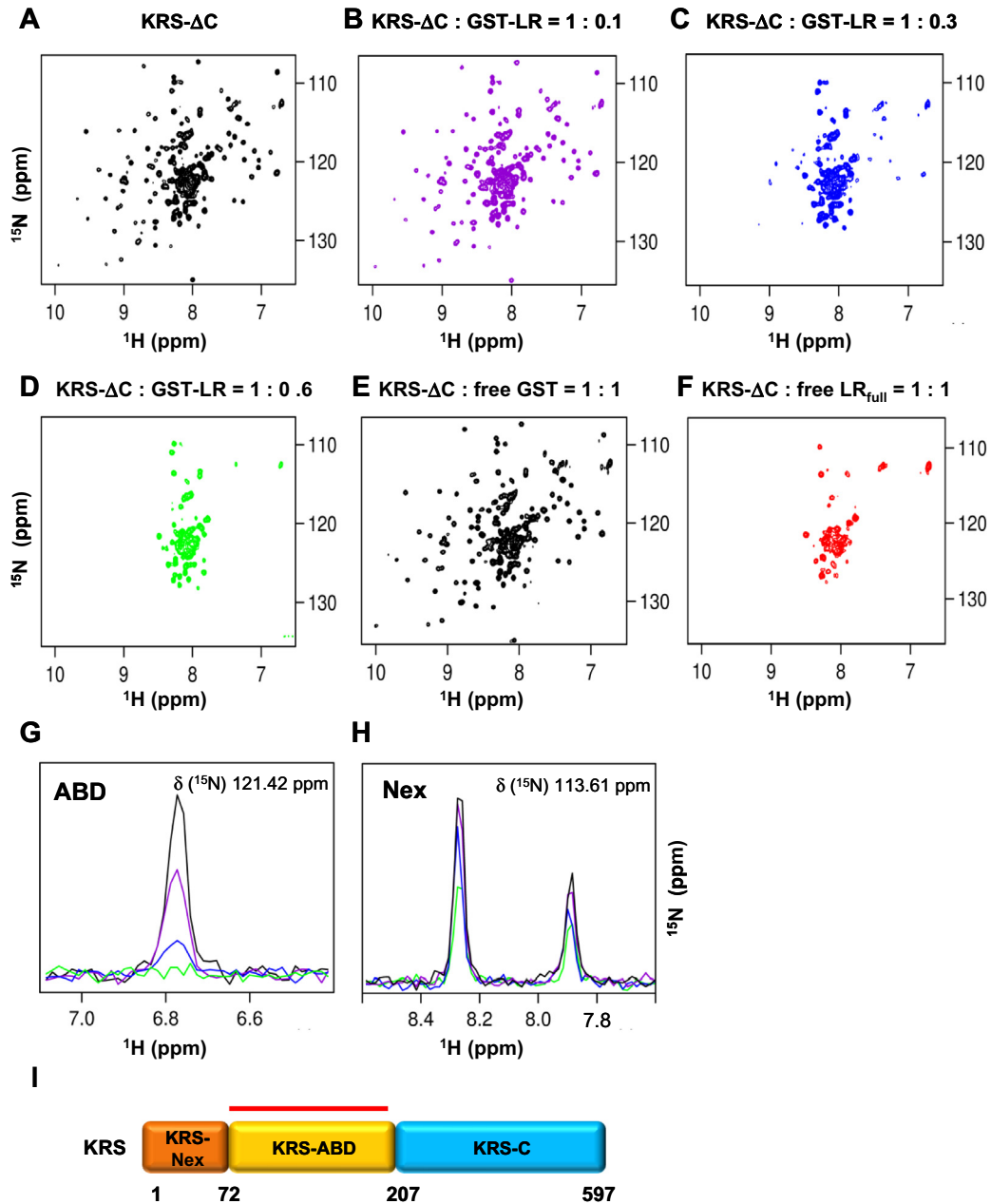


Fig. 1. Selective binding of 37LRP to the KRS anticodon-binding domain. ^1H - ^{15}N TROSY NMR spectra of ^{15}N -labeled KRS- ΔC with different ratios of GST-LR (A–D). (A) ^1H - ^{15}N TROSY spectrum of 0.2 mM KRS- ΔC (black). (B) ^1H - ^{15}N TROSY spectrum of 0.2 mM ^{15}N -labeled KRS- ΔC with 0.02 mM GST-LR (KRS- ΔC :GST-LR = 1:0.10) (purple). (C) ^1H - ^{15}N TROSY spectrum of 0.2 mM ^{15}N -labeled KRS- ΔC with 0.06 mM GST-LR (KRS- ΔC :GST-LR = 1:0.30) (blue). (D) ^1H - ^{15}N TROSY spectrum of 0.2 mM ^{15}N -labeled KRS- ΔC with 0.12 mM GST-LR (KRS- ΔC :GST-LR = 1:0.60) (green). (E) ^1H - ^{15}N TROSY spectrum of 0.2 mM ^{15}N -labeled KRS- ΔC with 0.2 mM free GST (KRS- ΔC :GST = 1:1) (black). (F) ^1H - ^{15}N TROSY spectrum of 0.2 mM ^{15}N -labeled KRS- ΔC with 0.2 mM tag-free LR_{full} (KRS- ΔC :LR_{full} = 1:1) (red). (G) Overlay of the 1-D cross-sections of the ^1H - ^{15}N TROSY spectra at 121.42 ppm (^{15}N) of different ratios of KRS- ΔC :GST-LR (KRS- ΔC [black], KRS- ΔC :GST-LR = 1:0.10 [purple], KRS- ΔC :GST-LR = 1:0.30 [blue], KRS- ΔC :GST-LR = 1:0.60 [green]). (H) Overlay of the 1-D cross-sections of ^1H - ^{15}N TROSY spectra at 113.61 ppm (^{15}N) of different ratios of KRS:GST-LR (KRS- ΔC [black], KRS- ΔC :GST-LR = 1:0.10 [purple], KRS- ΔC :GST-LR = 1:0.30 [blue], KRS- ΔC :GST-LR = 1:0.60 [green]). (I) Schematic diagram of the functional domains in human KRS. KRS has three functional domains: an N-terminal extension (KRS-Nex, residues 1–72), an anticodon-binding domain (KRS-ABD, residues 72–207), and a catalytic domain (KRS-C, residues 207–597). Residues 1–207 were termed KRS- ΔC . Red line denotes that the KRS-ABD is responsible for the 37LRP binding.

3.2. The anticodon-binding domain of KRS is responsible for the interaction with 37LRP

To investigate the mechanism of binding between KRS and LR, an NMR titration experiment was performed with KRS- ΔC and GST-LR. We monitored a series of ^1H - ^{15}N TROSY spectra of 0.2 mM ^{15}N -labeled KRS- ΔC to which GST-LR was added to give KRS- ΔC :GST-LR molar ratios of 1:0.10, 1:0.15, 1:0.30, 1:0.50, 1:0.60, 1:0.80, and 1:1.00. The NMR signals from the anticodon-binding domain of KRS (residues 72–207) were found to be

selectively and quantitatively decreased by binding with GST-LR, while the NMR signals from the N-terminal extension were only minimally affected (Fig. 1A–D). Free GST did not affect the NMR signals of KRS (Fig. 1E), and the addition of the tag-free 37 kDa LRP (tag-free LR_{full}) showed the similar result to that of GST-LR (Fig. 1F). Fig. 1G shows representative signals (corresponding to a residue Leu 115) from the anticodon-binding domain, indicating a dramatic decrease in the intensity upon titration. This dose-dependent decrease in the signal is thought to be a phenomenon associated with the formation of large-molecular weight complex

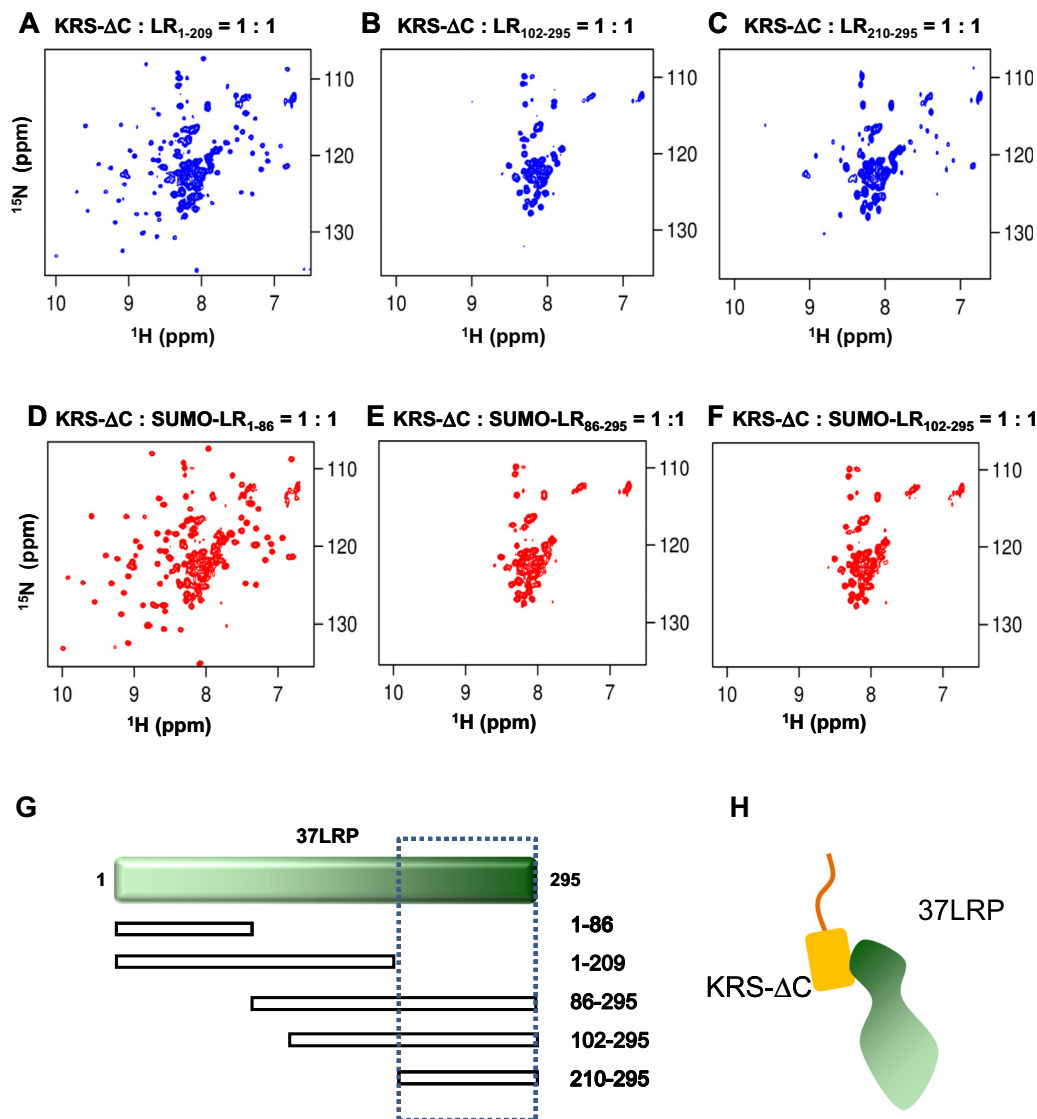


Fig. 2. The C-terminal region of 37LRP is responsible for the KRS binding. (A) ^1H - ^{15}N TROSY spectrum of 0.2 mM ^{15}N -labeled KRS-ΔC with 0.2 mM LR₁₋₂₀₉ (KRS-ΔC:LR₁₋₂₀₉ = 1:1) (blue). (B) ^1H - ^{15}N TROSY spectrum of 0.2 mM ^{15}N -labeled KRS-ΔC with 0.2 mM LR₁₀₂₋₂₉₅ (KRS-ΔC:LR₁₀₂₋₂₉₅ = 1:1) (blue). (C) ^1H - ^{15}N TROSY spectrum of 0.2 mM ^{15}N -labeled KRS-ΔC with 0.2 mM LR₂₁₀₋₂₉₅ (KRS-ΔC:LR₂₁₀₋₂₉₅ = 1:1) (blue). (D) ^1H - ^{15}N TROSY spectra of 0.2 mM ^{15}N -labeled KRS-ΔC with 0.2 mM SUMO-LR₁₋₈₆ (KRS-ΔC:SUMO-LR₁₋₈₆ = 1:1) (red). (E) ^1H - ^{15}N TROSY spectra of 0.2 mM ^{15}N -labeled KRS-ΔC with 0.2 mM SUMO-LR₈₆₋₂₉₅ (KRS-ΔC:SUMO-LR₈₆₋₂₉₅ = 1:1) (red). (F) ^1H - ^{15}N TROSY spectra of 0.2 mM ^{15}N -labeled KRS-ΔC with 0.2 mM SUMO-LR₁₀₂₋₂₉₅ (KRS-ΔC:SUMO-LR₁₀₂₋₂₉₅ = 1:1) (red). (G) Construct design of the 37LRP fragments for the binding study. An N-terminal region of 37LRP (LR₁₋₈₆, residues 1–86), exon 2–5 region (LR₁₋₂₀₉, residues 1–209, an $\alpha\beta$ domain with flavodoxin like fold), a computer-predicted transmembrane and C-terminal extracellular region (LR₈₆₋₂₉₅, residues 86–295) and a computer-predicted C-terminal extracellular region (LR₁₀₂₋₂₉₅, residues 102–295), exon 6–7 region (LR₂₁₀₋₂₉₅, residues 210–295). (H) Schematic representation of the interaction between KRS-ΔC and 37LRP. The anticodon-binding domain of KRS binds to the C-terminal region of 37LRP.

upon the binding of GST-LR and KRS-ΔC, or to be caused by chemical exchanges between the bound and unbound states. This indicates that the anticodon-binding domain of KRS is responsible for the binding to 37LRP (Fig. 1I). When the concentration ratio of KRS:GST-LR reached 1:0.6, most of the signals from the anticodon-binding domain disappeared. In contrast, for KRS:GST-LR ratios of up to 1:0.6, the intensity of the NMR signals from KRS-Nex (residues 1–72) were still at more than half of the original levels (Fig. 1H). Some signal broadening for KRS-Nex was observed, possibly because of the slow motion of the complex when compared to the free KRS-ΔC.

Purification of the complex of KRS-ABD and 37LRP was not successful due to the instability and aggregation of the complex. Although the individual solutions of KRS-ABD and TRX-LR were soluble in the experimental conditions, the binding of KRS-ABD

and TRX-LR induced co-precipitation in various buffer conditions of neutral pH and low salt concentrations under 400 mM NaCl (Supplemental Fig. 5). The addition of 20 mM arginine solubilized the KRS-ABD and TRX-LR complex (Supplemental Fig. 5C), allowing for NMR measurements of ^{15}N -labeled KRS-ABD with TRX-LR (1:1 ratio) to be carried out. The resulting spectra showed that the NMR signals of KRS-ABD completely disappeared following the addition of TRX-LR (Supplemental Fig. 3A and B). We further performed size exclusion chromatography to obtain the KRS-37LRP complex protein. We obtained some complex fractions eluted near void volume (Supplementary Fig. 6), although the proteins were degraded significantly. These findings further demonstrate that the anticodon-binding domain of KRS binds to 37LRP which results in signal broadenings in NMR experiments.

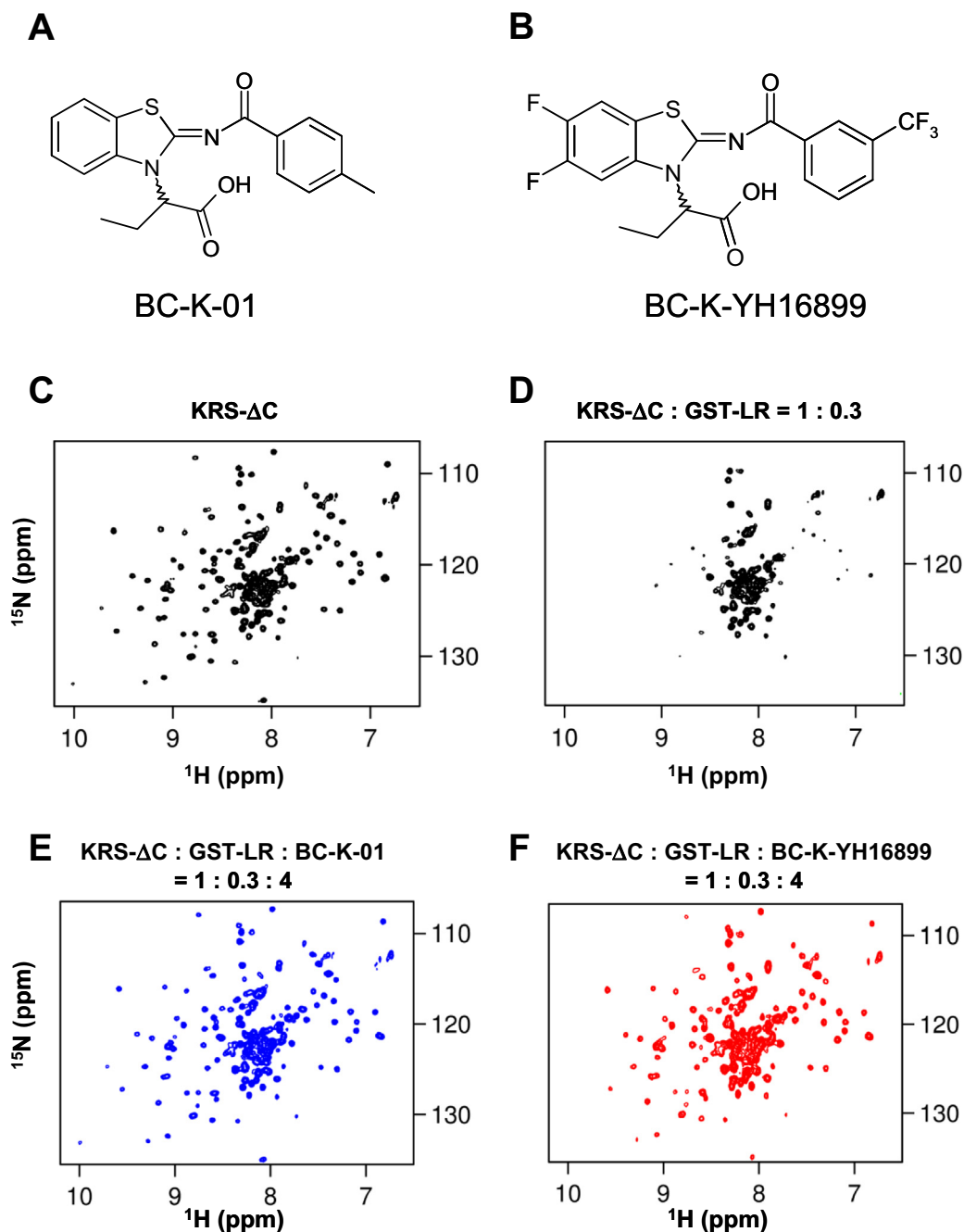


Fig. 3. Inhibitors compete with 37LRP at the KRS–LR binding interface. (A, B) Chemical structure of the inhibitor BC-K-01 (A) and its derivative BC-K-YH16899 (B). (C) ^1H - ^{15}N TROSY spectrum of ^{15}N -labeled 0.2 mM KRS- ΔC (black). (D) ^1H - ^{15}N TROSY spectrum of 0.2 mM ^{15}N -labeled KRS- ΔC with 0.06 mM GST-LR (black). (E) ^1H - ^{15}N TROSY spectrum of 0.2 mM ^{15}N -labeled KRS- ΔC with 0.06 mM GST-LR and 0.8 mM BC-K-01 (KRS- ΔC :GST-LR:BC-K-01 = 1:0.3:4) (blue). (F) ^1H - ^{15}N TROSY spectrum of 0.2 mM ^{15}N -labeled KRS- ΔC with 0.06 mM GST-LR and 0.8 mM BC-K-YH16899 (KRS- ΔC :GST-LR:BC-K-YH16899 = 1:0.3:4) (red).

3.3. The C-terminal region of 37LRP binds to the KRS anticodon-binding domain

Although the hypothetical model of LR with transmembrane region has been proposed by Castronovo et al. [28], this model has not been validated experimentally. Recently, the crystal structure of 37LRP has been reported for the N-terminal 220 residues, and this structure is $\alpha\beta$ flavodoxin-like fold comprising of 5–209 a.a. residues. In addition, ribosomal N-terminal region (residues 1–209) corresponds to exon 2–5 and metazoan-specific C-terminal region (residues 210–295) correspond to exon 6–7 suggest that these regions may be folded independently. Considering

these possibilities, and to identify the domain of 37LRP responsible for the binding to KRS, we expressed and purified the fragments of 37LRP (residues 1–295, LR_{full}; residues 1–86, LR_{1–86}; residues 1–102, LR_{1–102}; residues 1–209, LR_{1–209}; residues 86–295, LR_{86–295}; residues 102–295, LR_{102–295}; residues 210–295, LR_{210–295}) (Fig. 2G). All these constructs were expressed as SUMO-fused form and the SUMO tag was cleaved and removed during purification. Among them we could not purify the LR_{1–102} because it was not soluble.

A series of NMR spectra of ^{15}N -labeled KRS- ΔC with various 37LRP fragments (1:1 M ratio) were measured. As shown in Fig. 2A–C, selective signal broadening for the residues in the KRS

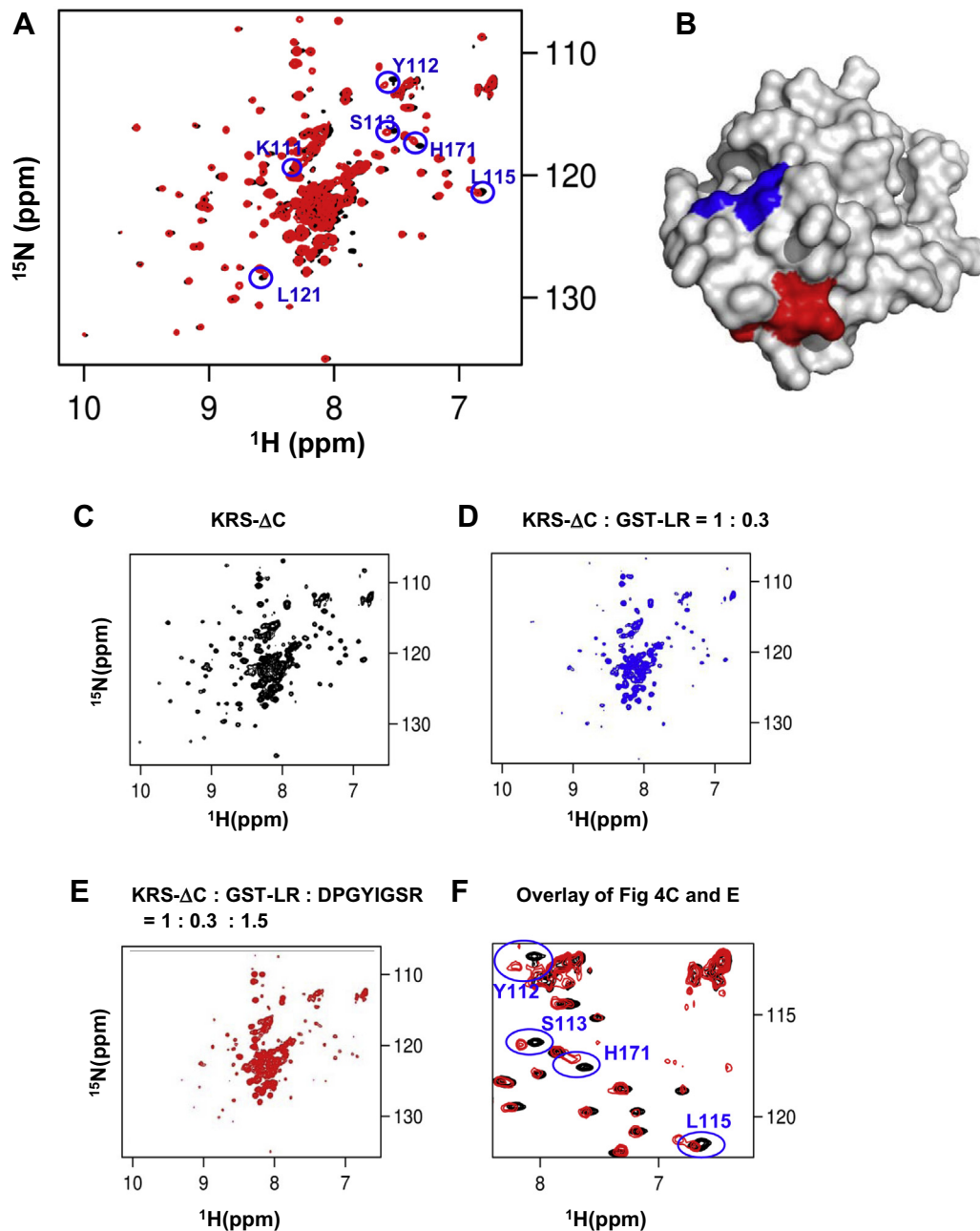


Fig. 4. Binding study of KRS anticodon-binding domain with laminin-derived peptide. (A) Superimposition of the 2D ^1H - ^{15}N TROSY spectra of 0.2 mM ^{15}N -labeled KRS- ΔC in the presence (red) and absence (black) of 0.3 mM laminin peptide. (B) Mapping of perturbed residues on the surface of the anticodon-binding domain of KRS. Significantly affected signals are shown in red. (C) ^1H - ^{15}N TROSY spectra of 0.2 mM ^{15}N -labeled KRS- ΔC (black). (D) ^1H - ^{15}N TROSY spectra of 0.2 mM ^{15}N -labeled KRS- ΔC with 0.06 mM GST-LR (KRS:GST-LR = 1:0.3) (blue). (E) ^1H - ^{15}N TROSY spectra of 0.2 mM ^{15}N -labeled KRS- ΔC with 0.06 mM GST-LR and 0.3 mM laminin peptide (KRS:GST-LR:laminin peptide = 1:0.3:1.5) (red). (F) An expanded region of the superimposed spectra of (C) and (E), showing the chemical shift perturbation of KRS- ΔC signals by the addition of laminin peptide.

anticodon-binding domain was observed in experiments with LR_{102–295} and LR_{210–295} (Fig. 2B and C), while that of LR_{1–209} did not show the selective broadening (Fig. 2A). Interestingly, the result in Fig. 2B is very similar to those of tag-free LR_{full} (Fig. 1F) and GST-LR (Fig. 1D), which indicates the C-terminal region of 37LRP is responsible for the binding to KRS. Addition of LR_{210–295} (Fig. 2C) showed weaker effect, but it still shows the selective signal broadening for anticodon-binding domain. For LR_{1–86}, we used SUMO-tagged form due to its instability after SUMO cleavage (Fig. 2D). To compare with this SUMO-tagged LR_{1–86}, we also present the NMR binding experiments with SUMO-LR_{86–295} and SUMO-LR_{102–295} (Fig. 2E and F), respectively. While SUMO-LR_{86–295}

(Fig. 2E) and SUMO-LR_{102–295} (Fig. 2F) showed similar pattern to those of tag-free LR_{full} (Fig. 1F) and GST-LR (Fig. 1D), SUMO-LR_{1–86} did not affect the NMR spectrum of KRS- ΔC . We were thus able to conclude that the anticodon-binding domain of KRS binds to the C-terminal region of 37LRP (Fig. 2H).

The K_d value of the interaction between KRS- ΔC and tag-free LR_{full}, as measured by surface plasmon resonance (SPR), was 40.4 μM (Supplemental Fig. 4A and B). In our setting, the KRS binding to 37LRP in vitro may be rather weaker than that in physiological condition, which is in 67LR form. In physiological condition, some other factors such as the laminin network and integrin molecules may also affect the KRS-LR binding resulting in the increase

of the affinity or stability of the complex. Notably, the binding affinity between KRS- Δ C and tag-free LR_{full} is weaker than the binding of BC-K-01 or BC-K-YH16899 to the KRS in our previous report [29], and thus these compounds appear to easily disrupt the KRS–37LRP interaction. These compounds are known to inhibit the interaction of KRS with LR and to suppress metastasis [29]. Intriguingly, the NMR signals of KRS- Δ C perturbed by the addition of GST-LR were recovered upon addition of the compounds BC-K01 or BC-K-YH16899 (Fig. 3). This result provides supporting evidence that these compounds directly inhibit the binding between KRS and 37LRP in vitro. These findings are in agreement with our previous report regarding the inhibitory effects of these compounds on the association between KRS and LR.

3.4. KRS interacts with both 37LRP and laminin

Laminin is a major protein in the basal lamina of most cells and tissues and plays a major role in cell migration and adhesion [20]. A laminin B1-derived peptide, DPGYIGSR, is known to be a functional motif that interacts with 67LR and that inhibits tumor growth and metastasis [30,31]. To determine whether this laminin peptide binds with KRS N-terminal region, we measured ¹H–¹⁵N TROSY spectra of ¹⁵N KRS- Δ C in the presence and absence of laminin peptide (DPGYIGSR). To our surprise, the addition of laminin peptide induced selective chemical shift perturbations of the KRS signals. The residues for which significant perturbation was observed include K111, Y112, S113, L115, L121, and H171 in anticodon-binding domain (Fig. 4A). To confirm this KRS–laminin binding takes place with full functional proteins, an SPR experiment with chip-bound full-length laminin exposed to increasing the concentration of KRS_{66–579} was performed. KRS_{66–579} construct containing anticodon-binding and catalytic domains was used due to the instability of full length KRS_{1–597}. We found that KRS_{66–579} binds to full-length laminin with *K_d* value of 8.9 μ M. (Supplemental Fig. 4C and D).

Then we added the laminin peptide into the KRS and 37LRP mixture to see whether the laminin peptide affect the binding of KRS to 37LRP or not. The addition of a molar excess of laminin peptide to the ¹⁵N-labeled KRS- Δ C and GST-LR mixture (KRS- Δ C:GST-LR:laminin peptide = 1:0.3:1.5) did not influence the linewidth of the KRS- Δ C signals significantly in ¹H–¹⁵N TROSY spectra (Fig. 4D and E); rather, it retains chemical shift perturbations of the KRS signals by the laminin peptide (Fig. 4F). This result indicates that laminin peptide does not interfere the binding of KRS to 37LRP, and also 37LRP does not interfere of the KRS binding to laminin peptide.

We mapped the perturbed signals on the surface of KRS-ABD with respect to the binding site for BC-K-YH16899 (Fig. 4B) [29]. Interestingly, the binding surface of KRS to laminin peptide is distinct from that of BC-K-YH16899, which suggests that KRS can bind simultaneously to both LR and laminin at the cell membrane, and that the binding of laminin to KRS does not interfere with the binding of LR to KRS.

4. Conclusion

NMR signals from the N-terminal extension and anticodon-binding domain in the KRS- Δ C protein were identified, and were found to closely match those from the individual domains, indicating that the two domains have independent motions. In addition, it was shown that the anticodon-binding domain of KRS is responsible for the interaction with the C-terminal region of LR, and this interaction is inhibited by the anti-metastasis compounds BC-K-01 and BC-K-YH16899. Beside the interaction with LR, KRS- Δ C binds to the laminin-derived peptide DPGYIGSR using the distinct surface from that of the inhibitor binding. This

interaction was confirmed by the SPR study using the functional proteins, KRS_{66–579} and full-length laminin. Together with the known interaction between laminin and LR, our results revealed the mechanism underlying the colocalization of KRS and LR on the cell surface, which in turn results in an increase in LR-mediated cancer cell migration and metastasis.

Acknowledgements

This work was supported by Global Frontier Project grants [NRF-M1AXA002-2010-0029785 and NRF-2013M3A6A4045160], and funded by Ministry of Science, ICP and Future Planning (MISP) of Korea.

Appendix A. Supplementary data

Supplementary data associated with this article can be found, in the online version, at <http://dx.doi.org/10.1016/j.febslet.2014.06.048>.

References

- Guo, M., Schimmel, P. and Yang, X.L. (2010) Functional expansion of human tRNA synthetases achieved by structural inventions. *FEBS Lett.* 584, 434–442.
- Park, S.G., Ewalt, K.L. and Kim, S. (2005) Functional expansion of aminoacyl-tRNA synthetases and their interacting factors: new perspectives on housekeepers. *Trends Biochem. Sci.* 30, 569–574.
- Park, S.G., Schimmel, P. and Kim, S. (2008) Aminoacyl tRNA synthetases and their connections to disease. *Proc. Natl. Acad. Sci. USA* 105, 11043–11049.
- Kim, S., You, S. and Hwang, D. (2011) Aminoacyl-tRNA synthetases and tumorigenesis: more than housekeeping. *Nat. Rev. Cancer* 11, 708–718.
- Kim, Y.W., Kwon, C., Liu, J.L., Kim, S.H. and Kim, S. (2012) Cancer association study of aminoacyl-tRNA synthetase signaling network in glioblastoma. *PLoS One* 7, e40960.
- Lee, S.W., Cho, B.H., Park, S.G. and Kim, S. (2004) Aminoacyl-tRNA synthetase complexes: beyond translation. *J. Cell Sci.* 117, 3725–3734.
- Park, S.G., Choi, E.C. and Kim, S. (2010) Aminoacyl-tRNA synthetase-interacting multifunctional proteins (AIMPs): a triad for cellular homeostasis. *IUBMB Life* 62, 296–302.
- Sampath, P. et al. (2004) Noncanonical function of glutamyl-prolyl-tRNA synthetase: gene-specific silencing of translation. *Cell* 119, 195–208.
- Guo, M., Ignatov, M., Musier-Forsyth, K., Schimmel, P. and Yang, X.L. (2008) Crystal structure of tetrameric form of human lysyl-tRNA synthetase: implications for multisynthetase complex formation. *Proc. Natl. Acad. Sci. USA* 105, 2331–2336.
- Ofir-Birin, Y. et al. (2013) Structural switch of lysyl-tRNA synthetase between translation and transcription. *Mol. Cell* 49, 30–42.
- Kang, T., Kwon, N.H., Lee, J.Y., Park, M.C., Kang, E., Kim, H.H., Kang, T.J. and Kim, S. (2012) AIMP3/p18 controls translational initiation by mediating the delivery of charged initiator tRNA to initiation complex. *J. Mol. Biol.* 423, 475–481.
- Yannay-Cohen, N. et al. (2009) LysRS serves as a key signaling molecule in the immune response by regulating gene expression. *Mol. Cell* 34, 603–611.
- Carmi-Levy, I., Yannay-Cohen, N., Kay, G., Razin, E. and Nechushtan, H. (2008) Diadenosine tetraphosphate hydrolase is part of the transcriptional regulation network in immunologically activated mast cells. *Mol. Cell Biol.* 28, 5777–5784.
- Lee, Y.N., Nechushtan, H., Figov, N. and Razin, E. (2004) The function of lysyl-tRNA synthetase and Ap4A as signaling regulators of MITF activity in Fc ϵ RI-activated mast cells. *Immunity* 20, 145–151.
- Kim, D.G. et al. (2012) Interaction of two translational components, lysyl-tRNA synthetase and p40/37LRP, in plasma membrane promotes laminin-dependent cell migration. *FASEB J.* 26, 4142–4159.
- Nechushtan, H., Kim, S., Kay, G. and Razin, E. (2009) Chapter 1: the physiological role of lysyl tRNA synthetase in the immune system. *Adv. Immunol.* 103, 1–27.
- Park, S.G., Kim, H.J., Min, Y.H., Choi, E.C., Shin, Y.K., Park, B.J., Lee, S.W. and Kim, S. (2005) Human lysyl-tRNA synthetase is secreted to trigger proinflammatory response. *Proc. Natl. Acad. Sci. USA* 102, 6356–6361.
- Guo, F., Gabor, J., Cen, S., Hu, K., Moulant, A.J. and Kleiman, L. (2005) Inhibition of cellular HIV-1 protease activity by lysyl-tRNA synthetase. *J. Biol. Chem.* 280, 26018–26023.
- Terranova, V.P., Rao, C.N., Kalebic, T., Margulies, I.M. and Liotta, L.A. (1983) Laminin receptor on human breast carcinoma cells. *Proc. Natl. Acad. Sci. USA* 80, 444–448.
- Nelson, J., McFerran, N.V., Pivato, G., Chambers, E., Doherty, C., Steele, D. and Timson, D.J. (2008) The 67 kDa laminin receptor: structure, function and role in disease. *Biosci. Rep.* 28, 33–48.
- Rea, V.E., Rossi, F.W., De Paulis, A., Ragno, P., Selleri, C. and Montuori, N. (2012) 67 kDa laminin receptor: structure, function and role in cancer and infection. *Infez. Med.* 20 (Suppl. 2), 8–12.

- [22] Buto, S. et al. (1998) Formation of the 67-kDa laminin receptor by acylation of the precursor. *J. Cell. Biochem.* 69, 244–251.
- [23] Jamieson, K.V., Wu, J., Hubbard, S.R. and Meruelo, D. (2008) Crystal structure of the human laminin receptor precursor. *J. Biol. Chem.* 283, 3002–3005.
- [24] Zidane, N., Ould-Abeih, M.B., Petit-Topin, I. and Bedouelle, H. (2013) The folded and disordered domains of human ribosomal protein SA have both idiosyncratic and shared functions as membrane receptors. *Biosci. Rep.* 33, 113–124.
- [25] Delaglio, F., Grzesiek, S., Vuister, G.W., Zhu, G., Pfeifer, J. and Bax, A. (1995) NMRPipe: a multidimensional spectral processing system based on UNIX pipes. *J. Biomol. NMR* 6, 277–293.
- [26] Vranken, W.F. et al. (2005) The CCPN data model for NMR spectroscopy: development of a software pipeline. *Proteins* 59, 687–696.
- [27] Francin, M., Kaminska, M., Kerjan, P. and Mirande, M. (2002) The N-terminal domain of mammalian Lysyl-tRNA synthetase is a functional tRNA-binding domain. *J. Biol. Chem.* 277, 1762–1769.
- [28] Castronovo, V., Tarabozetti, G. and Sobel, M.E. (1991) Functional domains of the 67-kDa laminin receptor precursor. *J. Biol. Chem.* 266, 20440–20446.
- [29] Kim, D.G. et al. (2014) Chemical inhibition of prometastatic lysyl-tRNA synthetase–laminin receptor interaction. *Nat. Chem. Biol.* 10, 29–34.
- [30] Iwamoto, Y., Robey, F.A., Graf, J., Sasaki, M., Kleinman, H.K., Yamada, Y. and Martin, G.R. (1987) YIGSR, a synthetic laminin pentapeptide, inhibits experimental metastasis formation. *Science* 238, 1132–1134.
- [31] Bushkin-Harav, I., Garty, N.B. and Littauer, U.Z. (1995) Down-regulation of a 67-kDa YIGSR-binding protein upon differentiation of human neuroblastoma cells. *J. Biol. Chem.* 270, 13422–13428.